Exploring the potential of leaf reflectance spectra for retrieving the leaf maximum carboxylation rate

Article *in* International Journal of Remote Sensing · February 2019

DOI: 10.1080/01431161.2019.1579940

CITATIONS
7

READS
317

4 authors:

Xiaojin Qian
Chinese Academy of Sciences
12 PUBLICATIONS **61** CITATIONS
SEE PROFILE

Yongjiang Zhang
Agricultural University Of Hebei
35 PUBLICATIONS **670** CITATIONS
SEE PROFILE

Liangyun Liu
Chinese Academy of Sciences
279 PUBLICATIONS **3,353** CITATIONS
SEE PROFILE

Shanshan Du
Chinese Academy of Sciences
18 PUBLICATIONS **262** CITATIONS
SEE PROFILE

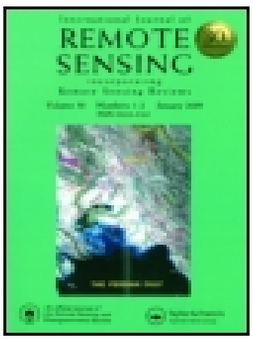

International Journal of Remote Sensing

ISSN: 0143-1161 (Print) 1366-5901 (Online) Journal homepage: https://www.tandfonline.com/loi/tres20

Exploring the potential of leaf reflectance spectra for retrieving the leaf maximum carboxylation rate

Xiaojin Qian, Yongjiang Zhang, Liangyun Liu & Shanshan Du

To cite this article: Xiaojin Qian, Yongjiang Zhang, Liangyun Liu & Shanshan Du (2019): Exploring the potential of leaf reflectance spectra for retrieving the leaf maximum carboxylation rate, International Journal of Remote Sensing, DOI: 10.1080/01431161.2019.1579940

To link to this article: https://doi.org/10.1080/01431161.2019.1579940

INTERNATIONAL JOURNAL OF REMOTE SENSING
https://doi.org/10.1080/01431161.2019.1579940

Taylor & Francis
Taylor & Francis Group

Exploring the potential of leaf reflectance spectra for retrieving the leaf maximum carboxylation rate

Xiaojin Qian[a,b], Yongjiang Zhang[c], Liangyun Liu [a] and Shanshan Du[a,b]

[a]Key Laboratory of Digital Earth Science, Institute of Remote Sensing and Digital Earth, Chinese Academy of Sciences, Beijing, China; [b]College of Resources and Environment, University of Chinese Academy of Sciences, Beijing, China; [c]College of Agronomy, Hebei Agricultural University/Key Laboratory of Crop Growth Regulation of Hebei Province, Baoding, China

ABSTRACT

The maximum carboxylation rate (V_{cmax}) is a key photosynthetic parameter that is determined by the leaf biochemistry and environmental conditions. Numerous studies have shown that plant biochemical, physiological and structural parameters can be estimated from reflectance spectra. Therefore, it is reasonable to assume that V_{cmax} can be spectrally determined. Here, we investigate the potential of leaf reflectance spectra for retrieving the maximum carboxylation rate of leaves. Measurements of leaf reflectance, carbon dioxide (CO_2) response curves, leaf chlorophyll-*a* + *b* (chl-*a* + *b*) etc., were made on 80 crop, shrub and tree leaves. Then, the leaf $V_{cmax,25}$ was linked to leaf biochemistry and spectral reflectance. A reliable relationship, with a coefficient of determination (R^2) value of 0.75, was found between the leaf chl-*a* + *b* content and $V_{cmax,25}$. The leaf $V_{cmax,25}$ values were also significantly correlated with chl-*a* + *b*-sensitive spectral indices with the highest R^2 value that was found being 0.83 for the ratio spectral index (RSI) using reflectances at 1089 nm and 695 nm. Finally, multiple stepwise regression (MSR) and a partial least-squares regression (PLSR) modelling approach were used to estimate $V_{cmax,25}$ from leaf reflectances. The results confirmed that $V_{cmax,25}$ can be reliably estimated from leaf reflectance spectra and give an R^2 value >0.80. These findings show that leaf chl-*a* + *b* can be used as a proxy for leaf $V_{cmax,25}$ and that leaf $V_{cmax,25}$ can be spectrally determined using leaf reflectance data.

ARTICLE HISTORY
Received 4 July 2018
Accepted 13 December 2018

1. Introduction

Terrestrial ecosystem models are powerful tools for exploring and simulating the land ecosystem carbon cycle (Zhou et al. 2014). Nowadays, most terrestrial ecosystem models take an enzyme kinetic model developed by Farquhar as their base for simulating photosynthesis (Farquhar, von Caemmerer, and Berry 1980). The maximum carboxylation rate (V_{cmax}) and the maximum electron transport rate (J_{max}) are two crucial parameters used as measures of leaf photosynthetic capacity. V_{cmax} is the maximum

CONTACT Liangyun Liu liuly@radi.ac.cn Key Laboratory of Digital Earth Science, Institute of Remote Sensing and Digital Earth, Chinese Academy of Sciences, Beijing, China

carboxylation rate catalyzed by the Rubisco enzyme in the carbon fixation reaction; that is, the maximum number of moles of carbon dioxide (CO_2) fixed per unit area of plant leaf per unit time (unit: μmol m^{-2} s^{-1}). V_{cmax} varies significantly with plant species, ranging from 6 to 194 μmol m^{-2} s^{-1} (Wullschleger 1993). In most classical biochemical models, V_{cmax} is either hypothesized as having a constant value for a given species or only the influence of temperature is considered (V_{cmax} is normalized to 25°C: $V_{cmax,25}$). Nevertheless, even for the same plant type, V_{cmax} varies significantly with location and season, which leads to large errors in simulations of photosynthesis. Therefore, the accurate acquisition of $V_{cmax,25}$ can help to accurately predict the photosynthetic capacity of plants and also facilitate the simulation of the carbon cycle for the global vegetation ecosystem.

As a key parameter of photosynthesis, the value of leaf V_{cmax} is inevitably determined by the leaf biochemistry and environmental conditions. Some studies have explored the relationships between V_{cmax} and leaf biochemical parameters. As a major constituent of the Rubisco and light-harvesting complexes that modulate photosynthesis, nitrogen has drawn most attention (Niinemets and Tenhunen 1997). Kattge et al. (2009) found that the mean $V_{cmax,25}$ for different plant function types (PFTs) was determined by the photosynthetic nitrogen-use efficiency and that the variation in $V_{cmax,25}$ was determined by the high variability of the leaf nitrogen content for each PFT. Dechant et al. (2017) demonstrated that the reflectance-based partial least-squares regression (PLS) models of $V_{cmax,25}$ were clearly based on the correlation with nitrogen content per unit area. However, retrieving leaf nitrogen over a large area has proved too challenging (Knyazikhin et al. 2013). Chlorophyll-*a* + *b* (chl-*a* + *b*) plays a key role in light harvesting in photosynthesis: this harvesting leads to the excitation of electrons, which then drives the production of nicotinamide adenine dinucleotide phosphate (NADPH) and chemical energy in the form of adenosine triphosphate (ATP) – these are used in the reactions of the photosynthetic carbon cycle (Croft et al. 2017). A strong linear relationship between chl-*a* + *b* and nitrogen within different species has been reported (Sage, Pearcy, and Seemann 1987; Evans 1989) and so some studies have attempted to explore the link between V_{cmax} and chl-*a* + *b*. Croft et al. (2017) investigated the use of biochemical parameters for modelling leaf photosynthetic capacity in a deciduous forest, showing that chl-*a* + *b* provides a more accurate, direct proxy for $V_{cmax,25}$. Houborg et al. (2015) indicated that chl-*a* + *b* could serve as an observational indicator of the value of $V_{cmax,25}$ and its seasonal variation, which is important for improved modelling of gross primary productivity (GPP). Luo et al. (2018) concluded that chl-*a* + *b* provided a reliable constraint on the seasonal variations in $V_{cmax,25}$ at a forest site and that the use of the chl-*a* + *b*-based $V_{cmax,25}$ in the terrestrial biosphere model (TBM) could significantly improve the precision of estimates of GPP and evapotranspiration (ET). The above studies found a good correlation between chl-*a* + *b* and $V_{cmax,25}$, but the effects of other biochemical contents on $V_{cmax,25}$ were barely clarified.

Although there is no specific spectral mechanism linking leaf V_{cmax} and the leaf spectral reflectance, the relationship between leaf V_{cmax} and some biochemical contents (such as nitrogen and chl-*a* + *b* content) can be employed to spectrally determine leaf V_{cmax}. Numerous studies have shown that plant biochemical, physiological and structural parameters can be spectrally determined at the leaf and canopy scale (Wu, Niu, and Gao 2012; Hunt et al. 2013; Soudani et al. 2014). Dechant et al. (2017) found that $V_{cmax,25}$ estimation using leaf reflectance was predominantly based on its relationship with the nitrogen

content per unit area. However, the characteristic bands related to leaf nitrogen are easily affected by cellular structure scattering and atmospheric water vapour (Herrmann et al. 2010), which makes it very challenging to retrieve leaf nitrogen from remote sensing data. The leaf chl-*a* + *b* can be reliably retrieved using spectral indices based on the red and near-infrared (NIR) bands. Several vegetation indices related to the red edge bands, such as GMI-2 (Gitelson and Merzlyak 1997), SR_{705}, ND_{705} (Gitelson and Merzlyak 1994), $CI_{red\ edge}$ (Gitelson et al. 2005) and mND_{705} (Sims and Gamon 2002), have shown excellent correlations with the chl-*a* + *b* content (Liu et al. 2017). In addition, leaf water content and leaf dry matter content (LMC), representing leaf biochemical components, can also successfully be derived from remote sensing reflectance spectra (Hunt and Rock 1989; Peñuelas et al. 1997; Liu et al. 2010; Féret et al. 2011; Wang et al. 2011).

There is no doubt that leaf V_{cmax} is determined by leaf biochemistry. The leaf reflectance spectra contain abundant leaf biochemical information. Numerous studies have shown that leaf biochemical components can be reliably retrieved from reflectance measurements. Therefore, it is reasonable to assume that the use of remotely sensed spectra, which are related to leaf biochemical components, can provide a promising new method of retrieving leaf $V_{cmax,25}$. However, so far, only a few studies have attempted to explore the direct link between leaf reflectance spectra and $V_{cmax,25}$. In this study, we explore the quantitative relationship between leaf biochemical components and $V_{cmax,25}$. More importantly, the specific objectives were to investigate the use of leaf spectra for estimating leaf $V_{cmax,25}$, and also to clarify the dominant mechanism behind the spectral method used to estimate leaf $V_{cmax,25}$.

2. Materials and methods

2.1. *Study sites and sampling*

Our research regions included a cotton test field in Baoding, Hebei province and the new technology campus of the Chinese Academy of Sciences, Beijing. Data were taken from a total of 80 leaves which included cotton, honeysuckle (*Lonicera japonica*), Chinese redbud (*Cercis chinensis*), forsythia (*Forsythia suspensa*), piemarker (*Abutilon theophrasti*) and white ash (*Fraxinus chinensis*). Detailed information about the samples is shown in Table 1. For each leaf, the photosynthetic CO_2 response curve, leaf reflectance, and leaf chl-*a* + *b* content were measured. Measurements were conducted during summer (July) and autumn (October) in 2017. The samples included crops, shrubs and trees and were chosen to represent as wide a range of leaf chl-*a* + *b* content as possible, with colours ranging from yellowish green to dark green. This was done in order to better investigate the relationships between leaf reflectance spectra and photosynthesis traits regardless of the plant type and leaf chl-*a* + *b* content.

Table 1. Information about the samples.

Species	Type	Number	Measurement date
Cotton	Crop	26	7 July–10 July 2017
Forsythia	Shrub	7	11 July 2017
Piemarker	Shrub	7	12 July 2017
White ash	Tree	14	12 October–13 October 2017
Honeysuckle	Shrub	16	12 October–13 October 2017
Chinese redbud	Shrub	10	14 October 2017

2.2. Gas exchange measurements and determination of $V_{cmax,25}$

Gas exchange measurements were carried out using the LI-6400 portable photosynthesis system (LI-COR, Lincoln, NE, USA). The measurements were made using a red/blue light source. The CO_2 response curves (A–Ci curves) were obtained under a photosynthetic photon flux density of 1500 µmol m^{-2} s^{-1} in July and 1000 µmol m^{-2} s^{-1} in October, with CO_2 concentrations of 400, 300, 200, 100, 50, 400, 400, 600, 900, 1200 and 1500 µmol CO_2 mol^{-1} air. Each step in the A–Ci curves lasted a minimum of 60 s and a maximum of 200 s. Throughout the measurements, the leaf temperature was kept constant close to the air temperature and the leaf relative humidity was kept the same as the relative humidity of the air. The values of the photosynthetic parameter, $V_{cmax,25}$, were calculated from the A–Ci curves using the R package 'plantecophys', a toolkit used to analyse and model leaf gas exchange data (Duursma 2015).

2.3. Leaf reflectance measurements

The leaf reflectance was measured in the field using an ASD FieldSpec Pro spectrometer (Analytical Spectral Devices Inc., Boulder, Colorado, USA), which was equipped with a fibre optic and the ASD plant probe. White reference measurements were performed before and after the measurements on the individual leaves. Mean reflectance spectra were calculated for each leaf by averaging the spectra obtained in five separate scans. The leaf reflectance was measured after the photosynthesis measurements in order to avoid potential physiological changes being induced by the high light intensity of the ASD plant probe (Dechant et al. 2017) or due to damage caused by the blade clip detector. Reflectance spectra for three types of leaves with the minimum and maximum chl-*a* + *b* content are shown in Figure 1. The higher the chl-*a* + *b* content, the smaller the green peak.

2.4. Estimation of leaf biochemical parameters

Three approaches were used for estimating the leaf chl-*a* + *b* content. The first approach was making soil and plant analyzer development (SPAD) measurements in the field. Leaf chl-*a* + *b* was measured non-destructively with a portable SPAD-502 chlorophyll meter (Konica Minolta Inc., Osaka, Japan). This instrument measures leaf transmittance at two wavelengths: red (650 nm), where there is strong absorption by chl-*a* + *b*, and near-infrared (940 nm), where there is no absorption by chl-*a* + *b*. The SPAD-502 meter calculates a unitless SPAD value (0–99) with a claimed accuracy of ±1 SPAD unit (Houborg et al. 2011). Markwell, Osterman, and Mitchell (1995) found that the SPAD-based model for chl-*a* + *b* is reliable for different plant species and obtained a coefficient of determination (R^2) value of 0.96 for their results. Therefore, in this study, the chl-*a* + *b* content was determined using the leaf SPAD value and calculated according to Equation (1):

$$\text{chl} - a + b \ \left(\mu\text{mol m}^{-2}\right) = 10.6 + 7.39 \times (\text{SPAD}) + 0.114 \times (\text{SPAD})^2 \quad (1)$$

The second approach was based on a leaf radiative transfer model (Fourty et al. 1996; Jacquemoud et al. 1996; Baret and Fourty 1997). A model of leaf optical properties spectra (PROSPECT-5B) allows leaf optical properties in the solar domain between 400 nm and 2500 nm (1 nm step) to be calculated. The input variables are the chl-*a* + *b* content, the

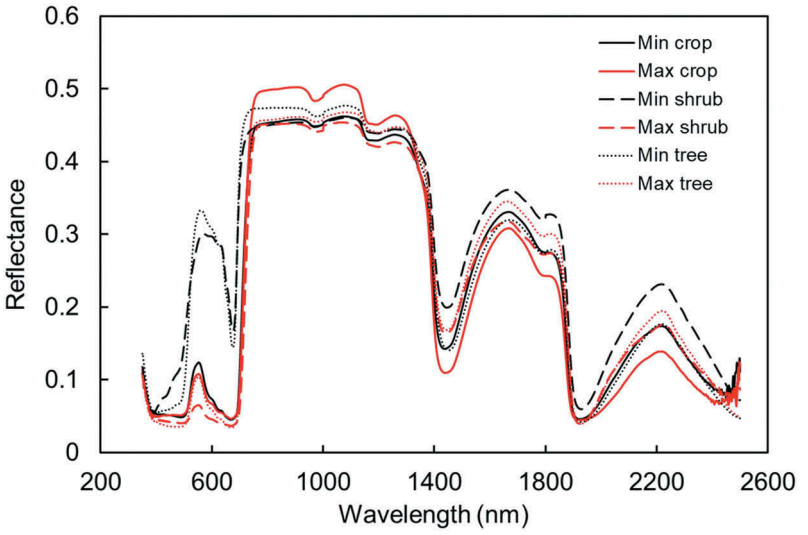

Figure 1. Reflectance spectra for three types of leaves with minimum and maximum chl-*a* + *b* content. The solid, dashed and dotted line represent crop, shrub and tree, respectively. The black line and red line represent the minimum and maximum chl-*a* + *b* content, respectively.

carotenoid content, the brown pigment content, the equivalent water thickness (EWT), the dry matter content, and the leaf structure parameter. The output variables are the leaf directional-hemispherical reflectance, and the transmittance. Here, we inverted PROSPECT-5B to retrieve leaf biochemical contents using the measured leaf spectral reflectance as input parameters (Jacquemoud and Baret 1990; Féret et al. 2008). The inversion consists of finding the parameter set (chl-*a* + *b* content, leaf structure parameter, EWT and LMC), symbolized by the θ, which minimizes the cost function:

$$J(\theta) = \sum_{\lambda_{min}}^{\lambda_{max}} \left(R^*(\lambda) - R_{mod}(\lambda, \theta)\right)^2 \tag{2}$$

Here, the scalar R^* consists of the measured reflectance values and R_{mod} the modelled ones. According to Féret et al. (2008), leaf biochemical contents, including the chl-*a* + *b* content, EWT and LMC, can be accurately retrieved using the above method.

The last method was based on the leaf reflectance measured in the field using the ASD spectrometer. It was found that the wavebands used for chl-*a* + *b* estimation are located in the near-infrared and red edge ranges. Thus, $CI_{red\ edge}$ and MTCI were adopted to build the chl-*a* + *b* model according to Equations (3)–(6) (Gitelson and Solovchenko 2017):

$$CI_{red\ edge} = (R_{NIR}/R_{red}) - 1 \tag{3}$$

$$MTCI = (R_{750} - R_{710})/(R_{710} - R_{680}) \tag{4}$$

$$\text{chl} - \text{a} + \text{b}\left(\mu\text{g cm}^{-2}\right) = 34.578 \times (CI)_{red\ edge} + 0.81 \tag{5}$$

$$\text{chl} - \text{a} + \text{b}\left(\mu\text{g cm}^{-2}\right) = 23.059 \times (MTCI) + 2.8841 \tag{6}$$

2.5. Sensitive bands and spectral indices

Sentinel-2 is an Earth observation mission developed by the European Space Agency (ESA) as part of the Copernicus Programme with the aim of carrying out terrestrial observations that support activities such as forest monitoring, land-cover change detection and natural disaster management. The Sentinel-2A satellite carries a single multispectral instrument (MSI), which has 13 spectral channels in the visible/near-infrared (VNIR) and shortwave infrared spectral range (SWIR). In order to assess the potential of using the reflectance spectra to estimate $V_{cmax,25}$ and provide some reference for the inversion of $V_{cmax,25}$ from canopy spectra, the field spectral data from the ASD spectrometer were aggregated to simulate the Sentinel-2A band settings using the spectral response functions (SRF) of MSI, according to Equation (7).

$$R_{rs}(b_i) = \frac{\int_{\lambda_m}^{\lambda_n} (\mathrm{SRF})(\lambda) \times R_{rs-meas}(\lambda) d\lambda}{\int_{\lambda_m}^{\lambda_n} (\mathrm{SRF})(\lambda) d\lambda} \quad (7)$$

where, the scalar $R_{rs}(b_i)$ denotes the simulated reflectance for the i-th band of the Sentinel-2A band settings, with integration from λ_m to λ_n for the i-th band; the scalar $R_{rs-meas}$ represents the reflectance as measured by the ASD spectrometer.

A spectral index is a non-dimensional index, usually a ratio or a linear or non-linear combination of the spectral reflectance of two or more bands, which compresses important information from a hyperspectral or multispectral dataset into a spectral index value. Previous studies have highlighted that estimates of leaf V_{cmax} can be made based on the correlation with leaf characteristics. In this study, we adopted a series of spectral indices calculated from leaf spectra to quantitatively evaluate the relationship between various biochemical components and $V_{cmax,25}$. Some popular spectral indices that are sensitive to chl-a + b, water content and LMC were also selected for estimating leaf $V_{cmax,25}$ (Inoue et al. 2016; Liu et al. 2017). The indices used are listed in Table 2.

Numerous studies have also shown that leaf traits can be accurately estimated from spectral indices. Given that the normalized difference spectral index (NDSI) and the ratio spectral index (RSI) are the standard ways of expressing the vegetation index, spectral reflectances in the range 400–2200 nm were combined into pairs and then all possible combinations of NDSI and RSI were linearly correlated to $V_{cmax,25}$ in this study.

2.6. Data analysis

Eighty groups of data were collected in this study. Sixty groups were randomly selected as the training dataset and the rest were used as the validation dataset. The following methods were employed to explore the potential of using leaf reflectance spectra to retrieve the leaf maximum carboxylation rate.

2.6.1. Partial correlation analysis

Partial correlation measures the degree of association between two random variables with the effect of a set of controlling random variables removed. When trying to find whether or to what extent there is a numerical relationship between two variables of interest, using the correlation coefficient for the relationship between them will give misleading results if there is

Table 2. Spectral indices sensitive to leaf biochemical components.

Biochemical component	Spectral index	Formula	References
Chlorophyll	RVI	R_{800}/R_{670}	(Pearson and Miller 1972)
	VOG-1	R_{740}/R_{720}	(Vogelmann, Rock, and Moss 1993)
	GMI-1	R_{750}/R_{550}	(Gitelson and Merzlyak 1997)
	GMI-2	R_{750}/R_{700}	
	SR_{705}	R_{750}/R_{705}	(Gitelson and Merzlyak 1994)
	ZM	R_{750}/R_{710}	(Zarco-Tejada et al. 2001)
	RI-1dB	R_{735}/R_{720}	(Gupta, Vijayan, and Prasad 2003)
	RI-2dB	R_{741}/R_{717}	
	RI-half	R_{747}/R_{708}	
	PRI	$(R_{531}-R_{570})/(R_{531}+R_{570})$	(Peñuelas, Filella, and Gamon 1995)
	GNDVI	$(R_{750}-R_{550})/(R_{750}+R_{550})$	(Gitelson and Merzlyak 1994)
	ND_{705}	$(R_{750}-R_{705})/(R_{750}+R_{705})$	
	NDVI	$(R_{810}-R_{680})/(R_{810}+R_{680})$	(Rouse et al. 1973)
	SAVI	$(1+0.5)\times(R_{810}-R_{680})/(R_{810}+R_{680}+0.5)$	(Huete 1988)
	$CI_{red\ edge}$	$R_{750}/R_{705}-1$	(Gitelson et al. 2005)
	CI_{green}	$R_{800}/R_{550}-1$	(Gitelson, Gritz, and Merzlyak 2003)
	mSR_{705}	$(R_{750}-R_{445})/(R_{705}-R_{445})$	(Sims and Gamon 2002)
	mND_{705}	$(R_{750}-R_{705})/(R_{750}+R_{705}-2\times R_{445})$	
	SIPI	$(R_{800}-R_{445})/(R_{800}-R_{680})$	(Peñuelas, Filella, and Gamon 1995)
	MCARI	$((R_{700}-R_{670})-0.2\times(R_{700}-R_{550}))\times(R_{700}/R_{670})$	(Daughtry et al. 2000)
	MTCI	$(R_{750}-R_{710})/(R_{710}-R_{680})$	(Dash and Curran 2004)
	EVI	$2.5\times(R_{860}-R_{645})/(1+R_{860}+6\times R_{645}-7.5\times R_{470})$	(Huete et al. 2002)
	VOG-2	$(R_{734}-R_{747})/(R_{715}+R_{726})$	(Vogelmann, Rock, and Moss 1993)
	VOG-3	$(R_{734}-R_{747})/(R_{715}+R_{720})$	
	λrep	$710+50\times((R_{810}+R_{660})/2-R_{710})/(R_{760}-R_{710})$	(Jongschaap and Booij 2004)
	RSI (D_{740}, D_{522})	D_{740}/D_{522}	(Inoue et al. 2012)
	CCI	D_{720}/D_{700}	(Sims et al. 2006)
Water	NDWI	$(R_{860}-R_{1240})/(R_{860}+R_{1240})$	(Gao 1996)
	WI	R_{900}/R_{970}	(Peñuelas et al. 1997)
	MSI	R_{1600}/R_{820}	(Hunt and Rock 1989)
	$REWT_{975}$	$-\ln(1-(1+a)(R_{945}-R_{975}))/k_{water\_975}$	(Liu et al. 2010)
LMC	NDLMA	$(R_{1368}-R_{1722})/(R_{1368}+R_{1722})$	(Féret et al. 2011)
	NDMI	$(R_{1649}-R_{1722})/(R_{1649}+R_{1722})$	(Wang et al. 20112011)

another variable that is numerically related to both variables of interest. This misleading situation can be avoided by controlling for the complicating variable, which can be done by computing the partial correlation coefficient. Because leaf chl-a + b, water content and LMC all have some relationship to $V_{cmax,25}$, we computed the partial correlation coefficients between the leaf biochemical components and $V_{cmax,25}$ to quantify their relationships.

2.6.2. *Multiple stepwise regression (MSR)*

Stepwise regression is a method of fitting regression models in which the choice of predictive variables is carried out automatically. In each step, a variable is considered for addition to or subtraction from the set of explanatory variables based on some prespecified criterion. The MSR ensures that only significant variables are included in the regression equation; that is, the final set of explanatory variables is the optimal one. However, there may be multicollinearity between variables, making models difficult to estimate accurately. Collinearity diagnosis of the optimal model was performed in this study. The variance inflation factor (VIF) is the ratio of the variance of a model with multiple terms to the variance of a model that has only one term. The VIF quantifies the severity of the multicollinearity in a regression analysis and provides an index that measures how much the variance (the square of the standard deviation of an estimate) of an estimated regression coefficient is increased because of collinearity. Empirical results

indicate that when $0 < VIF < 10$ there is no multicollinearity, when $10 \leq VIF < 100$ there is strong multicollinearity and when VIF≥100 there is serious multicollinearity. It is generally acknowledged that the predictive ability of models does not improve continuously as the number of variables increases. As independent variables that have little effect on the dependent variable are introduced into the regression equation, the stability of the parameter estimation can become weaker and the forecast error variance can increase. Therefore, 13 specific bands were used to build the MSR model for the $V_{cmax,25}$ estimation instead of all the bands in the 400–2500 nm range.

2.6.3. *Partial least-squares regression (PLSR)*

Partial least-squares regression (PLSR) is a statistical method that bears some relation to principal component regression. However, instead of finding hyperplanes of maximum variance between the response and independent variables, PLSR finds a linear regression model by projecting the predicted and observed variables into a new space. PLSR is particularly suitable when the matrix of predictors has more variables than observations and when there is multicollinearity between independent variables. In this study, the PLSR model was used to construct the relationships between $V_{cmax,25}$ and the 13 reflectance bands that were simulated.

3. Results

3.1. *Relationships between leaf biochemical components and $V_{cmax,25}$*

Figure 2 shows a comparison of the linear relationships between leaf chl-a + b content and $V_{cmax,25}$ for different methods of obtaining the chl-a + b content. The correlations between chl-a + b and leaf $V_{cmax,25}$ are strong, with the highest R^2 value being 0.75. Here, SPAD-based chl-a + b shows a relatively weak relationship mainly because of the measurement error.

Several studies have shown that $V_{cmax,25}$ is closely correlated with leaf biochemical components. The relationships were verified using eighty groups of data, as shown in Figure 3. The leaf chl-a + b content, EWT and LMC were all retrieved from the leaf reflectance using the PROSPECT-5B model. The strongest correlation is shown between leaf $V_{cmax,25}$ and chl-a + b (Pearson's correlation coefficient (r) = 0.859). The correlations between $V_{cmax,25}$ and EWT and LMC are weaker (r = 0.560 and r = 0.375, respectively).

Figure 3 shows the correlation between the leaf biochemical components and $V_{cmax,25}$. However, the relationships between the biochemical components can lead to interference regarding the dominant mechanism for the estimation of $V_{cmax,25}$. A partial correlation analysis between the leaf biochemical components and $V_{cmax,25}$ was also conducted. A significant linear relationship was found between $V_{cmax,25}$ and chl-a + b (r = 0.808). The correlations between $V_{cmax,25}$ and EWT (r = 0.219) and LMC (r = −0.302) were considerably weaker. These results proved that the leaf chl-a + b content was the dominant biochemical component that determines the leaf $V_{cmax,25}$.

3.2. *Relationships between leaf reflectance spectra and $V_{cmax,25}$*

The leaf reflectance was correlated with leaf $V_{cmax,25}$, as shown in Figure 4. The most significant correlation coefficient was −0.876 at 707 nm. The secondary significant wavelength was found at 549 nm (r = −0.854). The reflectances at the red edge position

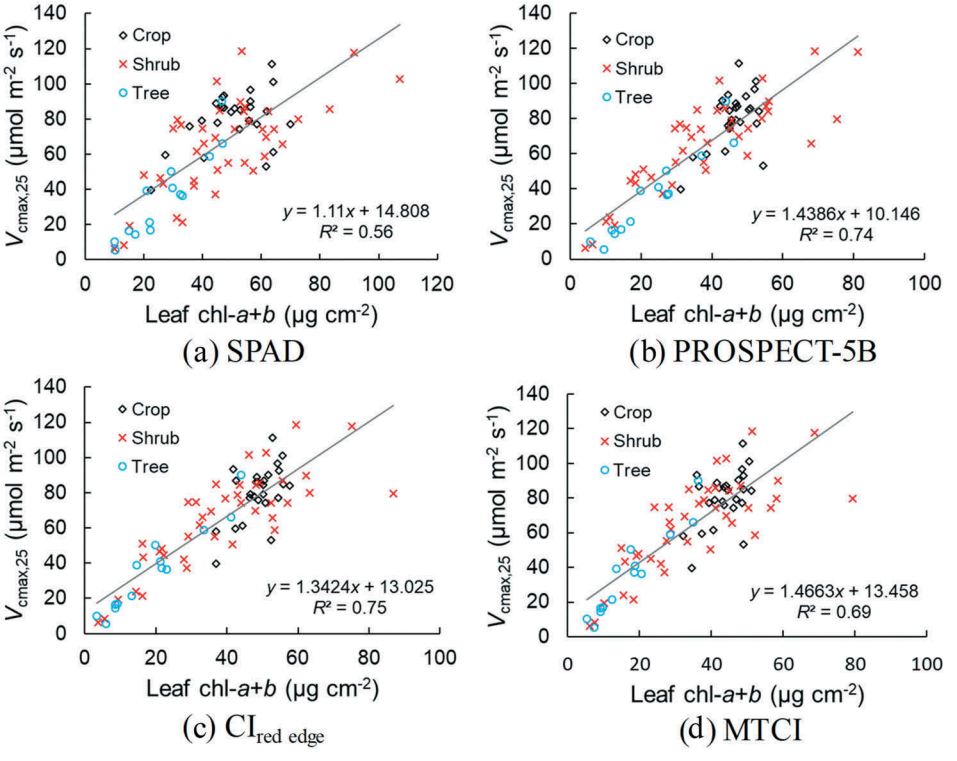

Figure 2. Relationships between $V_{cmax,25}$ and (a) SPAD-based leaf chl-*a* + *b*; (b) PROSPECT-5B-based leaf chl-*a* + *b*; (c) $CI_{red\ edge}$-based leaf chl-*a* + *b*; (d) MTCI-based leaf chl-*a* + *b*.

and the green peak were strongly and negatively correlated with $V_{cmax,25}$. There was a positive correlation between 775 and 1300 nm but the value of the correlation coefficient was relatively small. The low correlation was mainly affected by the leaf structure and was insensitive to the change in $V_{cmax,25}$. In addition, the characteristic nitrogen absorption band (SWIR) did not show a stronger relationship with $V_{cmax,25}$ either. The red edge contains abundant spectral information and is of great significance for the estimation of leaf parameters related to the pigment.

The corresponding values of the coefficients of determination (R^2) between $V_{cmax,25}$ and the spectral indices are shown in Figure 5. In the NDSI map (Figure 5a), the most significant spot (R^2 = 0.81) was found for NDSI (R_{705}, R_{1092}). Combinations of near-infrared bands with the 695–740 nm red edge band showed excellent predictive ability (R^2 > 0.70); the next best pairs were combinations of the 510–650 nm and near-infrared bands (R^2 > 0.60). Except for the water absorption wavelengths (around 1400 nm and 1900 nm), combinations of the wavelengths mentioned above (515–640 nm and 695–-710 nm) and the shortwave infrared bands had a moderate predictive ability. In the RSI map (Figure 5b), the most significant spot (R^2 = 0.82) was found around the peak of the RSI (R_{1089}, R_{695}). The distribution of values and also the trends in the RSI map are similar to those in the NDSI map, demonstrating that the sensitive bands for $V_{cmax,25}$ are robust. The red edge plays a critical role in the estimation of $V_{cmax,25}$ and has an excellent predictive ability if it is combined with near-infrared wavelengths.

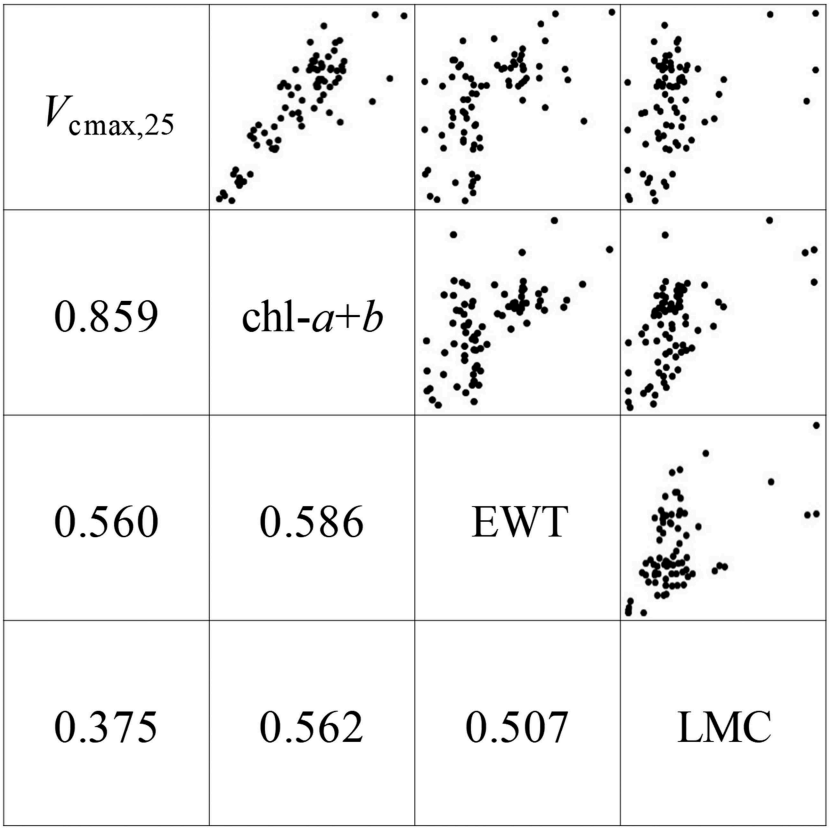

Figure 3. Correlations between maximum carboxylation rate ($V_{cmax,25}$), leaf chlorophyll-a + b content (chl-a + b), leaf equivalent water thickness (EWT) and dry matter content (LMC). The matrix of Pearson correlation coefficients between the measured leaf traits are shown below the diagonal. The corresponding scatter plots are shown above the diagonal.

Some popular spectral indices correlated with chl-a + b, water content and LMC were selected to test their ability to predict $V_{cmax,25}$, as shown in Figure 6. The $V_{cmax,25}$ models based on the RSI (R_{1089}, R_{695}) and NDSI (R_{705}, R_{1092}) ranked first and second in terms of predictive ability. It is noticeable that the RSI and NDSI using only two narrow wavebands had a very good predictive ability, giving an R^2 value >0.80 and a normalized RMSE (NRMSE = RMSE/range) value <0.12 even though only a linear model was used. Overall, the spectral indices sensitive to chl-a + b that use the red edge region, such as ND_{705}, GMI-2, mND_{705}, and SR_{705}, performed excellently. The spectral indices correlated with the water content and LMC did not show such a good predictive ability.

3.3. *Regression models for estimation of $V_{cmax,25}$*

3.3.1. *MSR model*

The 13 band reflectances that we simulated were used as independent variables to build an MSR model for the $V_{cmax,25}$ estimation. The five-element stepwise regression model based on the reflectance performed best, as illustrated by Equation (8) (R^2 = 0.85,

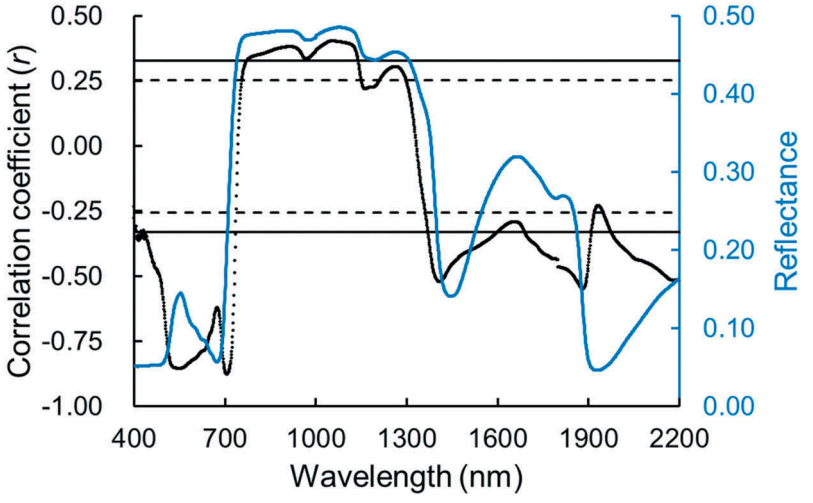

Figure 4. Correlation between $V_{cmax,25}$ and leaf reflectance. The dotted black line represents the linear correlation coefficient. The solid blue line represents the leaf reflectance. The dashed black line indicates that the correlation is significant at the 0.05 level. The solid black line indicates that the correlation is significant at the 0.01 level.

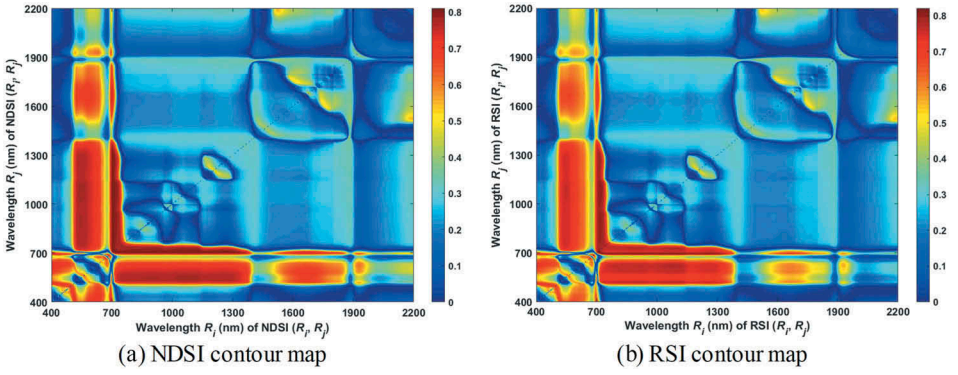

Figure 5. Contour maps of coefficients of determination (R^2) between $V_{cmax,25}$ and spectral indices based on two different wavelengths (λ_1, λ_2 nm).

NRMSE = 0.10). The results showed that the red edge region sensitive to chl-*a* + *b* was significant to the estimation of $V_{cmax,25}$ whereas the SWIR reported as being related to nitrogen was not significant. Diagnosis of the optimal model was also carried out as part of this study. In the optimal model, the values of the VIF for R_{705}, R_{945}, R_{740}, and R_{560} were all greater than 10, meaning that multicollinearity existed between the four variables.

$$V_{cmax,25}\left(\mu\text{mol m}^{-2}\text{s}^{-1}\right) = -677.120R_{705} + 734.983R_{945} - 673.822R_{740}$$

$$- 618.973R_{443} + 657.980R_{560} + 85.575 \quad (8)$$

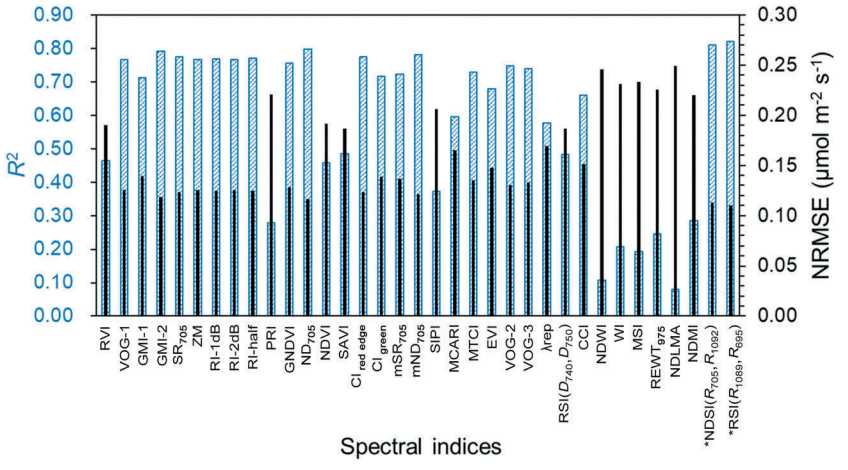

Figure 6. Performance of $V_{cmax,25}$ estimation models based on spectral indices in the training dataset. The blue columns represent the value of R^2. The black columns represent the value of NRMSE.

3.3.2. *PLSR model*

The PLSR modelling approach was also used to construct the relationships between $V_{cmax,25}$ and the 13 band reflectances that were simulated. Cross-validation with the PLSR modelling indicated that 80% of the $V_{cmax,25}$ variation could be explained by the model derived from the reflectance. Moreover, the $V_{cmax,25}$ model based on the PLSR could be considered reasonably accurate as its root mean square error was roughly 12% of the variable data range (R^2 = 0.80, NRMSE = 0.12).

3.4. *Validation of $V_{cmax,25}$ regression models*

The results in Section 3.3 indicate that the leaf photosynthesis trait $V_{cmax,25}$ can be accurately estimated from the leaf reflectance by applying the MSR and PLSR models to the training dataset. Several of the $V_{cmax,25}$ models that produced good estimates with the training dataset were assessed using the validation dataset, as shown in Table 3. The $V_{cmax,25}$ model based on RSI (R_{1089}, R_{695}), the new spectral index introduced in this paper, gave the best performance: its R^2 value was the highest (0.83) and NRMSE value the smallest (0.12). It was found that $V_{cmax,25}$ can be accurately estimated from the leaf reflectance spectra in the validation dataset giving an R^2 value >0.74 and an NRMSE value <0.15.

4. Discussion

4.1. *Relationships between leaf chl-a + b and $V_{cmax,25}$*

Previous studies have indicated that the leaf chl-*a* + *b* content can be used as a proxy for V_{cmax}. Croft et al. (2017) investigated the relationship using measurements made on four deciduous trees. The linear relationship between leaf chl-*a* + *b* and $V_{cmax,25}$ found in this study was also compared to that illustrated in Croft et al. (2017), as plotted in Figure 7.

Table 3. Performance of the models used to estimate $V_{cmax,25}$ with the validation dataset.

Model	Variable(s)	R^2	NRMSE
R-MSR	R_{705}, R_{945}, R_{740}, R_{443}, R_{560}	0.78	0.14
R-PLSR	13 wavebands	0.81	0.13
	GMI-2	0.80	0.13
	SR_{705}	0.77	0.14
	ND_{705}	0.79	0.13
SI-LR	$CI_{red\ edge}$	0.77	0.14
	mND_{705}	0.75	0.14
	*$NDSI(R_{705},R_{1092})$	0.77	0.14
	*$RSI(R_{1089},R_{695})$	0.83	0.12

R-MSR represents a multiple stepwise regression model based on the reflectance.
R-PLSR represents a partial least-squares regression model based on the reflectance.
SI-LR represents a linear regression model based on the spectral index.

The two leaf chl-*a* + *b*–$V_{cmax,25}$ models have very similar slopes, indicating a robust relationship between leaf chl-*a* + *b* content and $V_{cmax,25}$ across species and regions.

4.2. *Comparison of using leaf nitrogen and leaf chl-a + b content to estimate $V_{cmax,25}$*

Dechant et al. (2017) found a better correlation between leaf nitrogen per unit area and $V_{cmax,25}$ than between chl-*a* + *b* content and $V_{cmax,25}$. However, some studies have questioned the efficacy of the nitrogen-based method because the ratio of leaf nitrogen in the carboxylation system varies temporally due to the dynamic allocation of leaf nitrogen between the photosynthetic and non-photosynthetic components in leaves (Croft et al. 2017). Han et al. (2004) found that, for a given nitrogen value, $V_{cmax,25}$ differed by up to a factor of 2 between seasons. Compared with the total nitrogen content, the nitrogen content corresponding to the Rubisco enzyme can act as a proxy for leaf V_{cmax} (Croft et al. 2017). Unfortunately, it is too difficult to retrieve the Rubisco nitrogen content using remote sensing technology. As the Rubisco enzyme is found mainly in the chloroplast stroma, the chl-*a* + *b* content is closely related to the number of Rubisco enzymes (Clevers and Kooistra 2012; Schlemmer et al. 2013). Moreover, compared with the nitrogen content, the spectral response mechanism of the chl-*a* + *b* content in a leaf is clearer and is well modelled in vegetation radiation transfer models (Jacquemoud and Baret 1990). Also, there are far fewer limitations on the retrieval of chl-*a* + *b* than there are on the retrieval of nitrogen from satellite observations. Therefore, leaf chl-*a* + *b* is a better proxy than nitrogen for the estimation of V_{cmax} using remote sensing data.

4.3. *Mechanisms in the spectra-based estimation of $V_{cmax,25}$*

This study showed that the photosynthesis trait $V_{cmax,25}$ can be estimated from leaf reflectance spectra. The $V_{cmax,25}$ models using reflectance spectra outperformed the model using leaf chl-*a* + *b*. The locations of the $V_{cmax,25}$ measurements were not completely consistent with those of the chl-*a* + *b* measurements, which may have affected the results slightly. However, the leaf reflectance spectra contained the spectral absorption and scatter information of all the leaf biochemical contents, which may have been better correlated to leaf $V_{cmax,25}$ than the chl-*a*

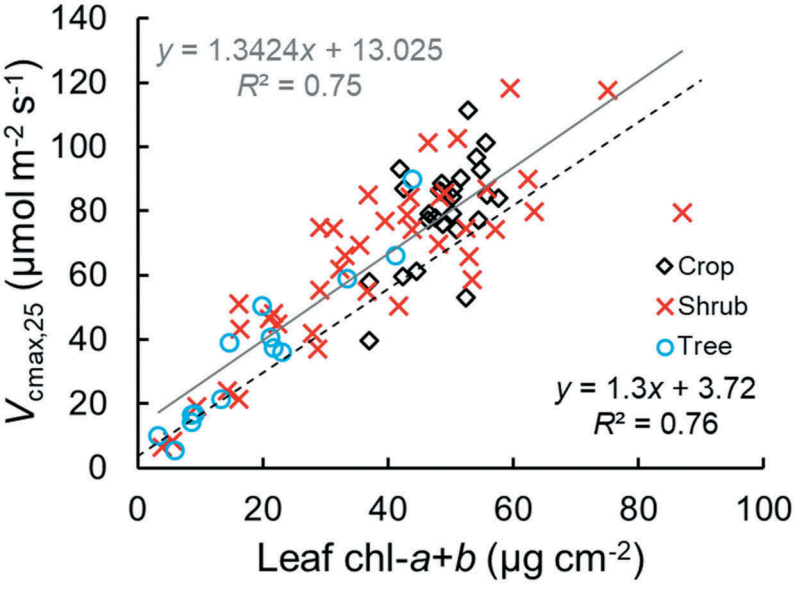

Figure 7. Relationships between leaf chl-*a* + *b* content and $V_{cmax,25}$. The dashed black line and solid grey line represent the relations between leaf chl-*a* + *b* content and $V_{cmax,25}$ in Croft et al. (2017) and as found in this study, respectively.

+ *b* content. Therefore, it is important to explore the relationship between the leaf biochemical components and $V_{cmax,25}$ if attempting to estimate $V_{cmax,25}$ from leaf reflectance spectra.

Table 4 shows the accuracy of the multiple linear regression (MLR) model used to estimate $V_{cmax,25}$ based on different combinations of leaf biochemical components retrieved from the leaf reflectance using the PROSPECT-5B model. When the water content was included, the accuracy of the estimation model increased slightly. That is to say, $V_{cmax,25}$ can be better estimated using a combination of chl-*a* + *b* and the water content. However, both the water content and the LMC contribute only a little to the estimates of $V_{cmax,25}$. Therefore, it can be concluded that the excellent estimates of leaf $V_{cmax,25}$ from leaf reflectance spectra are based on its strong correlation with the chl-*a* + *b* content.

5. Conclusions

The traditional method of obtaining leaf V_{cmax} using gas exchange measurements is tedious and time-consuming. It is extremely important to explore a new method to retrieve leaf V_{cmax} from remotely sensed data. In this study, the potential for using leaf reflectance spectra to retrieve leaf $V_{cmax,25}$ and the related mechanism were investigated.

Firstly, a reliable relationship between leaf chl-*a* + *b* content and $V_{cmax,25}$ was found (r = 0.859). The contributions of the water content and LMC to the estimates of $V_{cmax,25}$ were very small and could be neglected. In other words, chl-*a* + *b* content plays a dominant role in the spectral determination of $V_{cmax,25}$, which indicates a promising prospect for large-scale estimation of $V_{cmax,25}$ using remote sensing data.

Secondly, the leaf reflectance spectra were successfully employed to estimate leaf $V_{cmax,25}$. All the spectral indices sensitive to leaf chl-*a* + *b* content were significantly correlated with leaf $V_{cmax,25}$ – the highest R^2 value of 0.83 that was found was for RSI

Table 4. Performance of the models used to estimate $V_{cmax,25}$ based on different biochemical components.

	Training			Validation		
Model	R^2	RMSE (μmol m^{-2} s^{-1})	NRMSE	R^2	RMSE (μmol m^{-2} s^{-1})	NRMSE
MLR_{Chl}	0.72	13.11	0.12	0.81	8.78	0.11
$MLR_{Chl+Water}$	0.73	13.09	0.12	0.83	8.29	0.10
$MLR_{Chl+LMC}$	0.74	12.80	0.11	0.81	9.56	0.12
$MLR_{Chl+Water+LMC}$	0.75	12.68	0.11	0.84	8.81	0.11

MLR_* represents a multiple linear regression model based on different biochemical components (*).

(R_{1089}, R_{695}). The MSR and PLSR modelling approaches were also used to construct the relationships between $V_{cmax,25}$ and the leaf reflectance – in this case the highest R^2 value was 0.85. The results confirmed that the leaf photosynthesis trait, $V_{cmax,25,}$ could be accurately estimated from leaf reflectance spectra using both the training and validation datasets.

However, the number of plant species and samples collected in this study was still limited. Although our results agree well with Croft et al. (2017), more work should be carried out to investigate the mechanism in the spectral determination of leaf $V_{cmax,25}$. Furthermore, although our results indicate that the prospects for spectrally determining leaf $V_{cmax,25}$ at the leaf level are promising, there is still a big difference between this and making large-scale estimates of $V_{cmax,25}$ using satellite or airborne remote sensing data. Further studies should focus on the retrieval of leaf $V_{cmax,25}$ from canopy reflectance spectra observed using different platforms.

Disclosure statement

No potential conflict of interest was reported by the authors.

Funding

This work was supported by the National Key Research and Development Program of China [2017YFA0603001]; the National Natural Science Foundation of China [41671349]; Key Research Program of the Chinese Academy of Sciences [ZDRW-ZS-2019-1].

ORCID

Liangyun Liu http://orcid.org/0000-0002-7987-037X

References

Baret, F., and T. Fourty. 1997. "Estimation of Leaf Water Content and Specific Leaf Weight from Reflectance and Transmittance Measurements." *Agronomie* 17 (9–10): 455–464. doi:10.1051/agro:19970903.

Clevers, J. G. P. W., and L. Kooistra. 2012. "Using Hyperspectral Remote Sensing Data for Retrieving Canopy Chlorophyll and Nitrogen Content." *IEEE Journal of Selected Topics in Applied Earth Observations and Remote Sensing* 5 (2): 574–583. doi:10.1109/JSTARS.2011.2176468.

Croft, H., J. Chen, X. Luo, P. Bartlett, B. Chen, and R. M. Staebler. 2017. "Leaf Chlorophyll Content as a Proxy for Leaf Photosynthetic Capacity." *Global Change Biology* 23 (9): 3513–3524. doi:10.1111/gcb.13599.

Dash, J., and P. J. Curran. 2004. "The Meris Terrestrial Chlorophyll Index." *International Journal of Remote Sensing* 25 (23): 5403–5413. doi:10.1080/0143116042000274015.

Daughtry, C. S. T., C. L. Walthall, M. S. Kim, E. B. De Colstoun, and J. E. McMurtrey III. 2000. "Estimating Corn Leaf Chlorophyll Concentration from Leaf and Canopy Reflectance." *Remote Sensing of Environment* 74 (2): 229–239. doi:10.1016/S0034-4257(00)00113-9.

Dechant, B., M. Cuntz, M. Vohland, E. Schulz, and D. Doktor. 2017. "Estimation of Photosynthesis Traits from Leaf Reflectance Spectra: Correlation to Nitrogen Content as the Dominant Mechanism." *Remote Sensing of Environment* 196: 279–292. doi:10.1016/j.rse.2017.05.019.

Duursma, R. A. 2015. "Plantecophys-An R Package for Analysing and Modelling Leaf Gas Exchange Data." *PLoS One* 10 (11): e0143346. doi:10.1371/journal.pone.0143346.

Evans, J. R. 1989. "Photosynthesis and Nitrogen Relationships in Leaves of C_3 Plants." *Oecologia* 78 (1): 9–19. doi:10.1007/BF00377192.

Farquhar, G. D., S. von Caemmerer, and J. A. Berry. 1980. "A Biochemical Model of Photosynthetic CO_2 Assimilation in Leaves of C_3 Species." *Planta* 149 (1): 78–90. doi:10.1007/BF00386231.

Féret, J.-B., C. François, G. P. Asner, A. A. Gitelson, R. E. Martin, L. P. R. Bidel, S. L. Ustin, G. Le Maire, and S. Jacquemoud. 2008. "PROSPECT-4 and 5: Advances in the Leaf Optical Properties Model Separating Photosynthetic Pigments." *Remote Sensing of Environment* 112 (6): 3030–3043. doi:10.1016/j.rse.2008.02.012.

Féret, J.-B., C. François, A. Gitelson, G. P. Asner, K. M. Barry, C. Panigada, A. D. Richardson, and S. Jacquemoud. 2011. "Optimizing Spectral Indices and Chemometric Analysis of Leaf Chemical Properties Using Radiative Transfer Modeling." *Remote Sensing of Environment* 115 (10): 2742–2750. doi:10.1016/j.rse.2011.06.016.

Fourty, T., F. Baret, S. Jacquemoud, G. Schmuck, and J. Verdebout. 1996. "Leaf Optical Properties with Explicit Description of Its Biochemical Composition: Direct and Inverse Problems." *Remote Sensing of Environment* 56 (2): 104–117. doi:10.1016/0034-4257(95)00234-0.

Gao, B.-C. 1996. "NDWI—A Normalized Difference Water Index for Remote Sensing of Vegetation Liquid Water from Space." *Remote Sensing of Environment* 58 (3): 257–266. doi:10.1016/S0034-4257(96)00067-3.

Gitelson, A., and M. N. Merzlyak. 1994. "Quantitative Estimation of Chlorophyll-A Using Reflectance Spectra: Experiments with Autumn Chestnut and Maple Leaves." *Journal of Photochemistry and Photobiology B: Biology* 22 (3): 247–252. doi:10.1016/1011-1344(93)06963-4.

Gitelson, A., and A. Solovchenko. 2017. "Generic Algorithms for Estimating Foliar Pigment Content." *Geophysical Research Letters* 44 (18): 9293–9298. doi:10.1002/2017GL074799.

Gitelson, A. A., Y. Gritz, and M. N. Merzlyak. 2003. "Relationships between Leaf Chlorophyll Content and Spectral Reflectance and Algorithms for Non-Destructive Chlorophyll Assessment in Higher Plant Leaves." *Journal of Plant Physiology* 160 (3): 271–282. doi:10.1078/0176-1617-00887.

Gitelson, A. A., and M. N. Merzlyak. 1997. "Remote Estimation of Chlorophyll Content in Higher Plant Leaves." *International Journal of Remote Sensing* 18 (12): 2691–2697. doi:10.1080/014311697217558.

Gitelson, A. A., A. Vina, V. Ciganda, D. C. Rundquist, and T. J. Arkebauer. 2005. "Remote Estimation of Canopy Chlorophyll Content in Crops." *Geophysical Research Letters* 32 (8): 93–114. doi:10.1029/2005GL022688.

Gupta, R. K., D. Vijayan, and T. S. Prasad. 2003. "Comparative Analysis of Red-Edge Hyperspectral Indices." *Advances in Space Research* 32 (11): 2217–2222. doi:10.1016/S0273-1177(03)90545-X.

Han, Q., T. Kawasaki, T. Nakano, and Y. Chiba. 2004. "Spatial and Seasonal Variability of Temperature Responses of Biochemical Photosynthesis Parameters and Leaf Nitrogen Content within a Pinus Densiflora Crown." *Tree Physiology* 24 (7): 737–744. doi:10.1093/treephys/24.7.737.

Herrmann, I., A. Karnieli, D. J. Bonfil, Y. Cohen, and V. Alchanatis. 2010. "SWIR-Based Spectral Indices for Assessing Nitrogen Content in Potato Fields." *International Journal of Remote Sensing* 31 (19): 5127–5143. doi:10.1080/01431160903283892.

Houborg, R., M. C. Anderson, C. S. T. Daughtry, W. P. Kustas, and M. Rodell. 2011. "Using Leaf Chlorophyll to Parameterize Light-Use-Efficiency within a Thermal-Based Carbon, Water and Energy Exchange Model." *Remote Sensing of Environment* 115 (7): 1694–1705. doi:10.1016/j.rse.2011.02.027.

Houborg, R., M. F. McCabe, A. Cescatti, and A. A. Gitelson. 2015. "Leaf Chlorophyll Constraint on Model Simulated Gross Primary Productivity in Agricultural Systems." *International Journal of Applied Earth Observation and Geoinformation* 43: 160–176. doi:10.1016/j.jag.2015.03.016.

Huete, A., K. Didan, T. Miura, E. P. Rodriguez, X. Gao, and L. G. Ferreira. 2002. "Overview of the Radiometric and Biophysical Performance of the MODIS Vegetation Indices." *Remote Sensing of Environment* 83 (1–2): 195–213. doi:10.1016/S0034-4257(02)00096-2.

Huete, A. R. 1988. "A Soil-Adjusted Vegetation Index (SAVI)." *Remote Sensing of Environment* 25 (3): 295–309. doi:10.1016/0034-4257(88)90106-X.

Hunt, J. E. R., P. C. Doraiswamy, J. E. McMurtrey, C. S. T. Daughtry, E. M. Perry, and B. Akhmedov. 2013. "A Visible Band Index for Remote Sensing Leaf Chlorophyll Content at the Canopy Scale." *International Journal of Applied Earth Observation and Geoinformation* 21: 103–112. doi:10.1016/j.jag.2012.07.020.

Hunt, J. E. R., and B. N. Rock. 1989. "Detection of Changes in Leaf Water Content Using Near-And Middle-Infrared Reflectances." *Remote Sensing of Environment* 30 (1): 43–54. doi:10.1016/0034-4257(89)90046-1.

Inoue, Y., M. Guérif, F. Baret, A. Skidmore, A. Gitelson, M. Schlerf, R. Darvishzadeh, and A. Olioso. 2016. "Simple and Robust Methods for Remote Sensing of Canopy Chlorophyll Content: A Comparative Analysis of Hyperspectral Data for Different Types of Vegetation." *Plant, Cell & Environment* 39 (12): 2609–2623. doi:10.1111/pce.12815.

Inoue, Y., E. Sakaiya, Y. Zhu, and W. Takahashi. 2012. "Diagnostic Mapping of Canopy Nitrogen Content in Rice Based on Hyperspectral Measurements." *Remote Sensing of Environment* 126: 210–221. doi:10.1016/j.rse.2012.08.026.

Jacquemoud, S., and F. Baret. 1990. "PROSPECT: A Model of Leaf Optical Properties Spectra." *Remote Sensing of Environment* 34 (2): 75–91. doi:10.1016/0034-4257(90)90100-Z.

Jacquemoud, S., S. L. Ustin, J. Verdebout, G. Schmuck, G. Andreoli, and B. Hosgood. 1996. "Estimating Leaf Biochemistry Using the PROSPECT Leaf Optical Properties Model." *Remote Sensing of Environment* 56 (3): 194–202. doi:10.1016/0034-4257(95)00238-3.

Jongschaap, R. E. E., and R. Booij. 2004. "Spectral Measurements at Different Spatial Scales in Potato: Relating Leaf, Plant and Canopy Nitrogen Status." *International Journal of Applied Earth Observation and Geoinformation* 5 (3): 205–218. doi:10.1016/j.jag.2004.03.002.

Kattge, J., W. Knorr, T. Raddatz, and C. Wirth. 2009. "Quantifying Photosynthetic Capacity and Its Relationship to Leaf Nitrogen Content for Global-Scale Terrestrial Biosphere Models." *Global Change Biology* 15 (4): 976–991. doi:10.1111/j.1365-2486.2008.01744.x.

Knyazikhin, Y., M. A. Schull, P. Stenberg, M. Mõttus, M. Rautiainen, Y. Yang, A. Marshak, P. L. Carmona, R. K. Kaufmann, and P. Lewis. 2013. "Hyperspectral Remote Sensing of Foliar Nitrogen Content." *Proceedings of the National Academy of Sciences of the United States of America* 110 (3): E185–E192. doi:10.1073/pnas.1210196109.

Liu, L., B. Song, S. Zhang, and X. Liu. 2017. "A Novel Principal Component Analysis Method for the Reconstruction of Leaf Reflectance Spectra and Retrieval of Leaf Biochemical Contents." *Remote Sensing* 9 (11): 1113. doi:10.3390/rs9111113.

Liu, L., J. Wang, W. Huang, and C. Zhao. 2010. "Detection of Leaf and Canopy EWT by Calculating REWT from Reflectance Spectra." *International Journal of Remote Sensing* 31 (10): 2681–2695. doi:10.1080/01431160903085636.

Luo, X., H. Croft, J. Chen, P. Bartlett, R. Staebler, and N. Froelich. 2018. "Incorporating Leaf Chlorophyll Content into a Two-Leaf Terrestrial Biosphere Model for Estimating Carbon and Water Fluxes at a Forest Site." *Agricultural and Forest Meteorology* 248: 156–168. doi:10.1016/j.agrformet.2017.09.012.

Markwell, J., J. C. Osterman, and J. L. Mitchell. 1995. "Calibration of the Minolta Spad-502 Leaf Chlorophyll Meter." *Photosynthesis Research* 46 (3): 467–472. doi:10.1007/BF00032301.

Niinemets, Ü., and J. D. Tenhunen. 1997. "A Model Separating Leaf Structural and Physiological Effects on Carbon Gain along Light Gradients for the Shade-Tolerant Species Acer Saccharum." *Plant, Cell & Environment* 20 (7): 845–866. doi:doi:10.1046/j.1365-3040.1997.d01-133.x.

Pearson, R. L., and L. D. Miller. 1972. "Remote Mapping of Standing Crop Biomass for Estimation of the Productivity of the Shortgrass Prairie." Paper presented at the Remote Sensing of Environment, VIII, Ann Arbor, MI, October 2–6.

Peñuelas, J., I. Filella, and J. A. Gamon. 1995. "Assessment of Photosynthetic Radiation-Use Efficiency with Spectral Reflectance." *New Phytologist* 131 (3): 291–296. doi:10.1111/j.1469-8137.1995.tb03064.x.

Peñuelas, J., J. Pinol, R. Ogaya, and I. Filella. 1997. "Estimation of Plant Water Concentration by the Reflectance Water Index WI (R900/R970)." *International Journal of Remote Sensing* 18 (13): 2869–2875. doi:10.1080/014311697217396.

Rouse, J. J. W., R. H. Haas, J. A. Schell, and D. W. Deering. 1973. "Monitoring Vegetation Systems in the Great Plains with Erts."Paper presented at the Third ERTS-1 Symposium, Washington, DC, December 10–14.

Sage, R. F., R. W. Pearcy, and J. R. Seemann. 1987. "The Nitrogen Use Efficiency of C3 and C4 Plants: III. Leaf Nitrogen Effects on the Activity of Carboxylating Enzymes in Chenopodium Album (L.) And Amaranthus Retroflexus (L.)." *Plant Physiology* 85 (2): 355–359. doi:10.1104/pp.85.2.355.

Schlemmer, M., A. Gitelson, J. Schepers, R. Ferguson, Y. Peng, J. Shanahan, and D. Rundquist. 2013. "Remote Estimation of Nitrogen and Chlorophyll Contents in Maize at Leaf and Canopy Levels." *International Journal of Applied Earth Observation and Geoinformation* 25: 47–54. doi:10.1016/j.jag.2013.04.003.

Sims, D. A., and J. A. Gamon. 2002. "Relationships between Leaf Pigment Content and Spectral Reflectance across a Wide Range of Species, Leaf Structures and Developmental Stages." *Remote Sensing of Environment* 81 (2–3): 337–354. doi:10.1016/S0034-4257(02)00010-X.

Sims, D. A., H. Luo, S. Hastings, W. C. Oechel, A. F. Rahman, and J. A. Gamon. 2006. "Parallel Adjustments in Vegetation Greenness and Ecosystem CO_2 Exchange in Response to Drought in a Southern California Chaparral Ecosystem." *Remote Sensing of Environment* 103 (3): 289–303. doi:10.1016/j.rse.2005.01.020.

Soudani, K., G. Hmimina, E. Dufrêne, D. Berveiller, N. Delpierre, J.-M. Ourcival, S. Rambal, and R. Joffre. 2014. "Relationships between Photochemical Reflectance Index and Light-Use Efficiency in Deciduous and Evergreen Broadleaf Forests." *Remote Sensing of Environment* 144: 73–84. doi:10.1016/j.rse.2014.01.017.

Vogelmann, J. E., B. N. Rock, and D. M. Moss. 1993. "Red Edge Spectral Measurements from Sugar Maple Leaves." *International Journal of Remote Sensing* 14 (8): 1563–1575. doi:10.1080/01431169308953986.

Wang, L., E. R. Hunt, J. J. Jr, Q. X. Hao, and C. S. T. Daughtry. 2011. "Towards Estimation of Canopy Foliar Biomass with Spectral Reflectance Measurements." *Remote Sensing of Environment* 115 (3): 836–840. doi:10.1016/j.rse.2010.11.011.

Wu, C., Z. Niu, and S. Gao. 2012. "The Potential of the Satellite Derived Green Chlorophyll Index for Estimating Midday Light Use Efficiency in Maize, Coniferous Forest and Grassland." *Ecological Indicators* 14 (1): 66–73. doi:10.1016/j.ecolind.2011.08.018.

Wullschleger, S. D. 1993. "Biochemical Limitations to Carbon Assimilation in C_3 Plants—A Retrospective Analysis of the A/Ci Curves from 109 Species." *Journal of Experimental Botany* 44 (5): 907–920. doi:10.1093/jxb/44.5.907.

Zarco-Tejada, P. J., J. R. Miller, T. L. Noland, G. H. Mohammed, and P. H. Sampson. 2001. "Scaling-Up and Model Inversion Methods with Narrowband Optical Indices for Chlorophyll Content Estimation in Closed Forest Canopies with Hyperspectral Data." *IEEE Transactions on Geoscience and Remote Sensing* 39 (7): 1491–1507. doi:10.1109/36.934080.

Zhou, Y., W. Ju, X. Sun, Z. Hu, S. Han, T. A. Black, R. S. Jassal, and X. Wu. 2014. "Close Relationship between Spectral Vegetation Indices and V_{cmax} in Deciduous and Mixed Forests." *Tellus B: Chemical and Physical Meteorology* 66 (1): 23279. doi:10.3402/tellusb.v66.23279.